Catalytic Antibodies Induced by a Zwitterionic Hapten

Takeshi Tsumuraya,*[a] Nobuo Takazawa,[a] Atsuko Tsunakawa,[a] Roman Fleck,[b] and Satoru Masamune*[b]

Abstract: A zwitterionic hapten **4** featuring both positively and negatively charged functional groups was designed and synthesized with the goal of generating catalytic antibodies for the hydrolysis of ester **6** and amide **7**. Of the 36 monoclonal antibodies specific to BSA–**4** (bovine serum albumin) that were isolated, six accelerated the hydrolysis of **6**. Two catalytic antibodies with distinctively different and representative kinetic behaviors were selected for detailed kinetic studies. Whereas H8-2-6F11 showed burst kinetic behavior, which can be attributed to the formation of an acyl intermediate, H8-1-2D5 did not, but it did exhibit high multiple turnover activity. The rate of hydrolysis of **6** catalyzed by H8-1-2D5 followed Michaelis–Menten kinetics; the apparent values of the Michaelis–Menten constant K_m and the catalytic constant k_{cat} were 488 μM and 3.5 min^{-1}, respectively. The catalytic rate enhancement (k_{cat}/k_{un}) observed for H8-1-2D5 was 1.3×10^5, which is approximately two orders of magnitude greater than those for monofunctional haptens. Thus H8-1-2D5 compares well in catalytic activity with antibodies isolated by a related approach called heterologous immunization.

Keywords: catalytic antibodies · haptens · immunochemistry · kinetics · transition states

Introduction

Since antibody catalysts were first reported,[1] a large number of catalytic antibodies have been prepared for a wide variety of chemical transformations ranging from esterolysis to pericyclic reactions.[2] Initial studies on the generation of hydrolytic antibodies focused on phosphonate haptens that mimic the tetrahedral geometry of the transition state.[2–5] However, rate accelerations achieved by these catalytic antibodies were, in most cases, several orders of magnitude lower than those realized by their natural enzyme counterparts.[4] Clearly, achievement of further rate enhancement is an important and challenging task to enable practical application of catalytic antibodies.

According to the concept of reactive immunization (one emerging approach to boosting antibody performance), haptens used for immunization form a covalent bond with the antibody.[6] This method has yielded very efficient antibodies capable of catalyzing aldol and hydrolytic reactions. Moreover, recent advances in X-ray structure analysis of catalytic antibodies have greatly improved our understanding of the mechanism of hydrolytic antibodies.[7]

In our recent efforts to generate more efficient esterolytic antibodies by inducing both acidic and basic side-chain residues in the antibody combining site, analogously to aspartic proteases,[8, 9a] we devised a heterologous immunization strategy, whereby mice were immunized sequentially with two structurally related but differently functionalized haptens **1** and **2**.[9b–d] This method yielded antibodies capable of hydrolyzing ester **3** up to a hundredfold more efficiently than a homologous immunization protocol using only one of these haptens.

A complementary strategy for the generation of multiply charged residues in the antibody combining site may be to use a zwitterionic hapten that incorporates both negatively and positively charged functionalities. However, the synthesis of such a bifunctional hapten is usually more challenging than that of the monofunctional haptens generally used for the generation of catalytic antibodies. We now report the successful synthesis of a stable, zwitterionic hapten **4**, which has been designed to induce catalytic antibodies capable of hydrolyzing ester **6** and amide **7**. It has been used to generate catalytic antibodies that have been characterized kinetically and thermodynamically. These experiments allowed us to compare the two strategies, heterologous immunization and immunization with a zwitterionic hapten.

[a] Dr. T. Tsumuraya,[+] N. Takazawa, A. Tsunakawa
Kao Institute for Fundamental Research
2606 Akabane, Ichikaimachi, Haga, Tochigi 321-3497 (Japan)

[b] Prof. Dr. S. Masamune, Dr. R. Fleck
Department of Chemistry
Massachusetts Institute of Technology
Cambridge, Massachusetts 02139 (USA)
Fax: (+1) 617-253-1340
E-mail: masamune@mit.edu

[+] Present address: Department of Bioorganic Chemistry
Biomolecular Engineering Research Institute
6-2-3 Furuedai, Suita, Osaka 565-0874 (Japan)
Fax: (+81) 6-6872-8219
E-mail: tsumu@beri.co.jp

  0947-6539/01/0717-3748 $ 17.50+.50/0

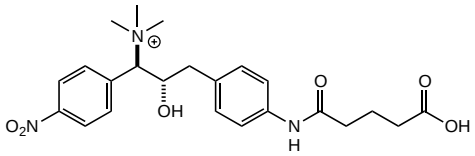

1

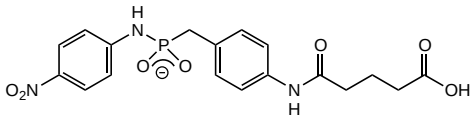

2

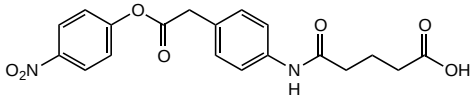

3

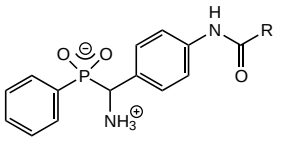

4 (R = CH_2CH_2SH)
5 (R = $CH_2CH_2CH_2COOH$)
5a (R = CH_3)

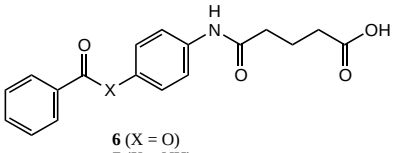

6 (X = O)
7 (X = NH)

lize the oxyanion of the transition state. The tetrahedral geometry of the phosphinate also serves as an isosteric replacement for the transition state. 2) The protonated α-amino functionality is intended to induce a basic residue in the active site, which is expected to deprotonate a water molecule in order to transform it into a hydroxide (a better nucleophile). The amino group may also generate a cavity for the incoming water molecule, thereby positioning it appropriately for the nucleophilic attack.

Hapten **4** was synthesized in six steps from commercially available *p*-nitrobenzaldehyde (Scheme 1). The aminophosphinic acid skeleton of **4** was constructed by aminoalkylation of *p*-nitrobenzaldehyde with dichlorophenylphosphine and benzylcarbamate,[10] and subsequent hydrolysis provided phosphinic acid **8**. Esterification of the phosphinate followed by selective reduction of the nitro group with $NaBH_4$ and $NiCl_2$ yielded the aminophosphinic acid methyl ester **10**. EDC-mediated (EDC = 1-ethyl-3-(3-dimethylaminopropyl)-carbodiimide) coupling of **10** with 3,3′-dithiopropionic acid afforded **11** as a mixture of diastereomers. Treatment of disulfide **11** with trimethylsilyl iodide hydrolyzed both the phosphinate ester and the carbamate, thus deprotecting the α-amino and the phosphinic acid groups. Finally, reduction of the disulfide bond with dithioerythritol (DTE) gave good yields of **4**. Hapten **4** was coupled to maleimide-activated keyhole limpet hemocyanin (KLH) and bovine serum albumin (BSA) through its thiol residue. Conjugate KLH–**4** was used for immunizations and conjugate BSA–**4** was used for subsequent enzyme-linked immunosorbent assays (ELISA).

Results and Discussion

Hapten design, synthesis, and antibody production: Zwitterionic hapten **4** was designed to induce acidic and/or basic amino acid residues in the antibody combining site by charge complementarity (Figure 1). The α-amino phosphinate moiety in **4** exhibits two distinct features. 1) The phosphinate is expected to induce an acidic residue in the catalytic site that would stabi-

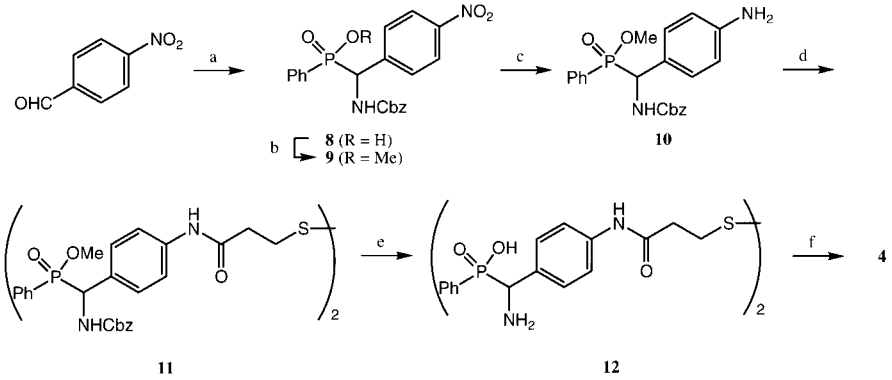

8 (R = H)
9 (R = Me)

10

11

12

Scheme 1. Synthesis of hapten **4**. Reagents and conditions: a) H_2N-CO_2Bn, $PhPCl_2$, acetic acid, reflux, 81%; b) EDC, DMAP, MeOH/DMSO, reflux, 90%; c) $NaBH_4/NiCl_2$, RT, MeOH, 34%; d) $(S(CH_2)_2COOH)_2$, EDC, $CHCl_3$, RT, 33%; e) i) TMSI, 2-methyl-2-butene, acetonitrile, RT; ii) MeOH, RT, 91% in two steps; f) DTE, $CHCl_3$, RT, 98%.

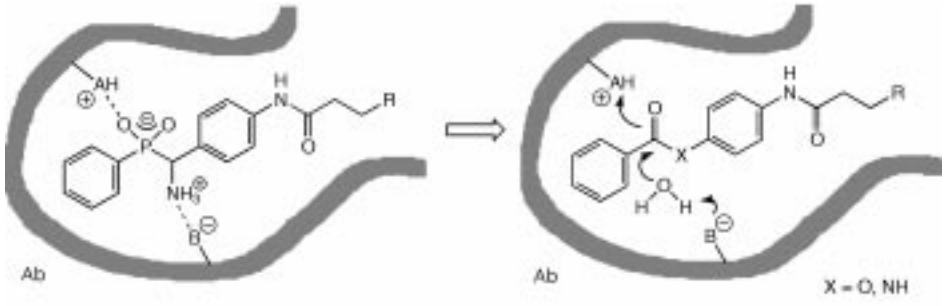

Figure 1. Schematic drawing of an antibody combining site elicited against hapten **4**.

For inhibition studies, a more water-soluble hapten that contained a glutaric acid linker was synthesized (Scheme 2). Synthesis of inhibitor **5** from **8** was analogous to that of hapten **4**. Selective reduction of the nitro group of **8** with hydrazine and a catalytic amount of palladium on carbon gave the aminophosphinic acid **13**, which

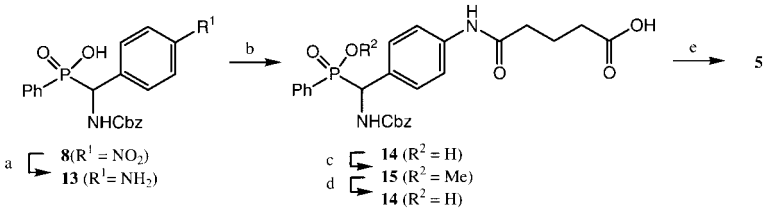

Scheme 2. Synthesis of inhibitor **5**. Reagents and conditions: a) $H_2N–NH_2$, 10% Pd/C, EtOH, reflux, 82%; b) glutaric anhydride, DMAP, pyridine, 87%; c) EDC, CH_2Cl_2/MeOH, 52%; d) LiOH, H_2O, THF, RT, 99%; e) H_2, 10% Pd/C, MeOH, RT, 97%.

was treated with glutaric anhydride to yield crude **14**. To facilitate purification of the final inhibitor, **14** was transiently converted into its dimethyl ester **15** by using EDC in methanol. Basic hydrolysis of **15** with LiOH followed by hydrogenolysis provided pure **5** in excellent yield.

Balb/c mice were immunized three times with KLH–**4** and 36 monoclonal antibodies were prepared according to standard protocols.[11, 12]

Thermodynamic and kinetic properties of antibodies: The 36 monoclonal antibodies ([Ab] = 10 μM) were screened for their ability to hydrolyze the ester substrate **6** in a buffered solution at three different pH values (50 mM Mes, 80 μM NaCl, pH 6.2; 50 mM HEPES, 80 μM NaCl, pH 7.8; 50 mM 2-(cycloamino)-ethanesulfonic acid (CHES), 80 μM NaCl, pH 9.0) containing dioxane (5%). The production of the phenol derivative **16** was

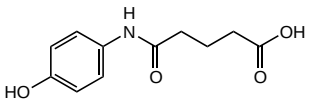

16

monitored by HPLC. Six of these monoclonal antibodies accelerated the hydrolysis of **6**, but no appreciable rate acceleration of the cleavage of the amide bond in **7** was observed.

All the catalytic antibodies were characterized further and found to obey Michaelis–Menten kinetics for the hydrolysis of **6**. The first-order rate constants (k_{cat}), the Michaelis–Menten constants (K_m), the dissociation constants (K_d) of all the catalytic antibodies, and the inhibition constants (K_i) of two representative ones, H8-1-2D5 and H8-2-6F11, were determined (Table 1). The background rate of hydrolysis of substrate **6** (k_{un}) is 2.67×10^{-5} min^{-1}, which compares well with those of other unactivated esters. However, we chose an aromatic ester as substrate as we expected the antibodies to use the phenolic moiety as an additional recognition element.

The binding affinities of all the antibodies to **5** were determined by competitive ELISA.[13, 14] As expected, the K_d values of the antibodies against **5**, which lay in the range 10^{-9}–10^{-4} M typically observed for antibody–antigen binding, indicated tight binding. The increased catalytic activity of the six antibodies, however, does not correlate with increased binding affinity to **5**. For example, the most active catalytic antibody, H8-1-2D5, shows a moderate affinity ($K_d = 1.7 \times 10^{-7}$ M) for **5**, whereas the tightest binding antibody, H8-1-3C4 ($K_d = 6.1 \times 10^{-9}$ M), does not accelerate the hydrolysis of ester **6**. A similar lack of correlation between catalytic activity and hapten affinity has been observed previously.[5g]

Further characterization of catalytic antibodies: The six catalytic antibodies can be classified into two groups on the basis of their kinetic behavior. H8-1-4H5, H8-1-6D2, and H8-2-6F11 exhibited burst kinetic behavior, whereas the other three, H8-1-2D5, H8-1-3G6, and H8-1-4D6, showed no burst phase but did show high multiple turnover numbers (vide infra). One representative catalytic antibody from each group, H8-1-2D5 and H8-2-6F11, were studied further in detail.

Table 1. Michaelis–Menten parameters and dissociation constants of catalytic antibodies.[a]

Antibody	k_{cat} [min^{-1}]	K_m [μM]	K_d for **5** [M][b]	K_i for **5** [nM][c]	k_{cat}/k_{un}
H8-1-2D5	3.5	488	1.7×10^{-7}	1.6	130000
H8-1-3G6	8.5×10^{-3}	375	1.1×10^{-7}		320
H8-1-4D6	1.9×10^{-2}	293	6.6×10^{-8}		710
H8-1-4H5	0.14	1100	2.1×10^{-7}		5200
H8-1-6D2	0.17	2100	1.1×10^{-7}		6400
H8-2-6F11	0.18	35.6	3.3×10^{-6}	17	6700

[a] The Michaelis–Menten kinetic parameters for the catalytic antibodies were determined in 50 mM HEPES, 80 μM NaCl, pH 7.8 at 37 °C. The background hydrolysis without antibody was determined by an initial rate analysis with extrapolation to zero buffer concentration ($k_{un} = 2.67 \times 10^{-5}$ min^{-1}). All assays were performed in duplicate. See the Experimental Section for details. [b] Determined by competitive ELISA in PBS. See the Experimental Section of ref. [9a] for details of this method. [c] Determined by fitting the data to Equation (1) as described in the text.

H8-1-2D5: This antibody showed the highest catalytic activity, and the rate of hydrolysis of **6** catalyzed by H8-1-2D5 followed Michaelis–Menten kinetics (Figure 2). Apparent

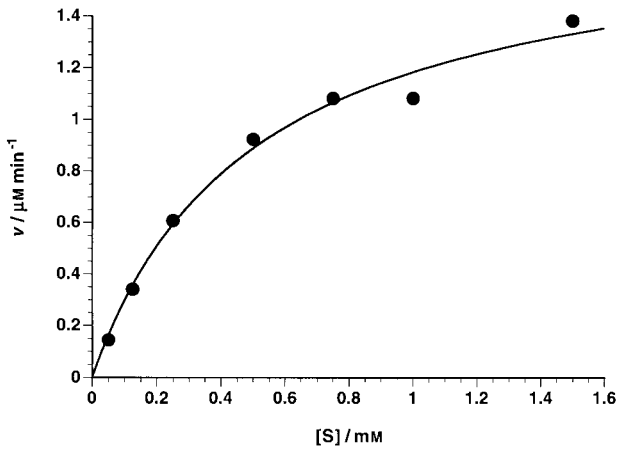

Figure 2. Michaelis–Menten plot for the hydrolysis of **6** catalyzed by H8-1-2D5 (0.5 μM). Assays were performed at 37 °C in 50 mM HEPES, 80 μM NaCl, pH 7.8. The data were corrected for the buffer-catalyzed background reaction, measured under the same conditions. The curve was fitted to the Michaelis–Menten equation [Eq. (4) in the text].

0947-6539/01/0717-3750 $ 17.50+.50/0 *Chem. Eur. J.* **2001**, *7*, No. 17

values for k_{cat} and K_m at pH 7.8 (50 mM HEPES, 80 μM NaCl) were 3.5 min^{-1} and 488 μM, respectively, and rate acceleration k_{cat}/k_{un} was 1.3×10^5, which was at least two orders of magnitude greater than for the catalytic antibodies raised against related monofunctional haptens **17** and **18** (Table 2).[5a,b] No significant product inhibition was observed, resulting in actual turnover numbers greater than 500.

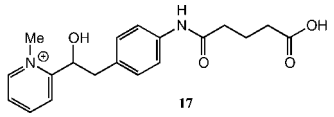

17

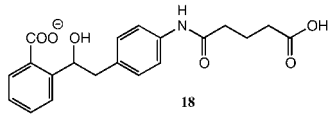

18

Table 2. Kinetic parameters for the antibody-catalyzed hydrolysis of ester **6**.

Antibody	Hapten	pH	k_{cat} [min^{-1}]	K_m [μM]	Ref.
H8-1-2D5	**4**	7.8	3.5	488	this work
	4	8.5	6.0	388	this work
	4	7.2	1.2	370	this work
30C6	**17**	7.2	0.005	1120	[5a]
27A6	**18**	8.5	0.01	243	[5b]

Several control experiments demonstrated that the efficiency of the esterolytic activity was not due to a contaminating enzyme. 1) F_{ab} fragments of H8-1-2D5 prepared by papain digestion were found to exhibit hydrolytic activity indistinguishable from that of the parent antibody. 2) Equally active antibodies were obtained from several different batches of ascites or hybridoma. Repeated purification of antibodies by different methods (protein G affinity chromatography, anti-mouse IgG + IgM affinity chromatography, and monoQ anion exchange chromatography) did not affect catalytic rates. 3) The catalytic activity of H8-1-2D5 was competitively inhibited by addition of **5** (vide infra).

Catalytic antibody H8-1-2D5 demonstrated competitive tight-binding inhibition by inhibitor **5** (Table 1 and Figure 3). K_i for **5** was determined at a fixed substrate concentration ($2K_m = 976$ μM) by fitting the initial rate v_0 to the equation for tight-binding inhibition [Eq. (1)], where v is the initial rate in the presence of inhibitor **5**, v_0 is the initial rate in the absence of **5**, E is the concentration of functional catalyst, I is the concentration of **5**, K_i' is the apparent inhibition constant defined by Equation (2), and S ($= 2K_m$) is the substrate concentration.[15]

$$v = \{(v_0/2E)[E - I - K_i' + (K_i' + I - E)^2 + 4EK_i']^{1/2} \quad (1)$$

$$K_i' = K_i(1 + S/K_m) \quad (2)$$

The K_i value for inhibitor **5** derived from Equations (1) and (2) was 1.6 nM, suggesting strongly that catalytic activity is associated with binding in the antibody combining site.

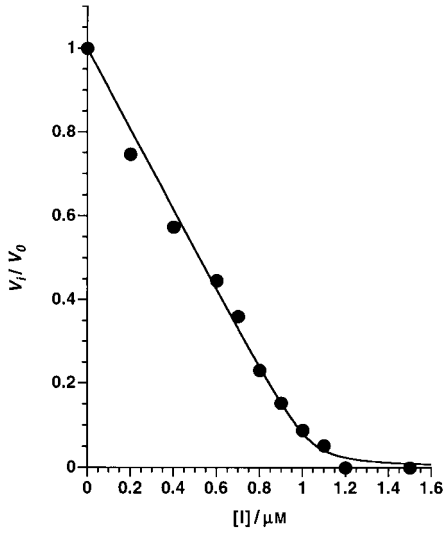

Figure 3. Tight-binding inhibition of antibody H8-1-2D5 by **5**. Initial rates were measured at increasing concentrations of **5** in the presence of H8-1-2D5 (0.5 μM) and **6** (976 μM), and the curve was fitted to Equations (1) and (2) as described in the text.

A series of chemical modifications were carried out to identify the amino acid residues involved in the catalytic process. Treatment of H8-1-2D5 with phenylglyoxal (which modifies arginine residues)[16] or diethyl pyrocarbonate (which modifies histidine residues)[17] resulted in complete loss of catalytic activity. However, after the same treatment in the presence of inhibitor **5a**, antibody H8-1-2D5 retained 80% of its activity. Nitration of tyrosine residues with tetranitromethane[18] reduced the esterolytic activity by 84%, whereas treatment of the antibody with glycine ethyl ester in the presence of EDC showed only a small effect (8% loss of activity). These results are consistent with catalytically active arginine and histidine residues in the antibody combining site. Histidine may function as a general base, while arginine stabilizes the developing negative charge of the transition state.[19]

H8-2-6F11: Antibody H8-2-6F11 exhibited a characteristic single-turnover pre-steady-state kinetic burst (Figure 4). The progressive curve fitted well to Equation (3), in which k is the observed apparent first-order rate constant of the decrease in the rate of catalysis, V_0 is the initial rate, and V_f is the steady-state rate.

$$[P] = V_f t + [(V_0 - V_f)(1 - \exp(-kt))]/k \quad (3)$$

The Michaelis–Menten parameters were determined for initial and steady-state rates V_0 and V_f, both of which follow Michaelis–Menten kinetics (Figure 5). For V_0 $k_{cat} = 9.2 \times 10^{-2}$ min^{-1} and $K_m = 35.6$ μM, and for V_f $k_{cat} = 1.6 \times 10^{-2}$ min^{-1}, $K_m = 168$ μM. H8-2-6F11 was also strongly inhibited by the addition of **5** (K_i = 17 nM).

The burst behavior of H8-2-6F11 was unchanged by addition of the reaction products (**16** or benzoic acid), so it cannot be accounted for by product inhibition. It could be explained, however, by the formation and significant accumulation of an acyl intermediate. Similar results were

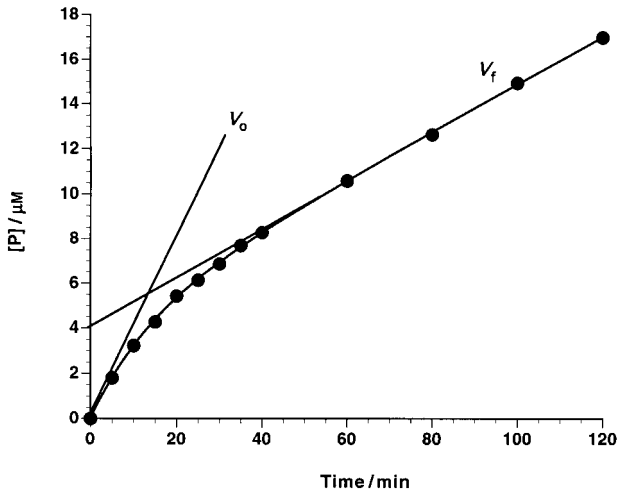

Figure 4. Formation of 5-[(4-hydroxyphenyl)amino]-5-oxopentanoic acid (**16**) during the hydrolysis of ester **6** (500 μM) catalyzed by antibody H8-2-6F11 (2 μM) at pH 7.8. The curves indicate the fit of data to Equation (3) by nonlinear regression.

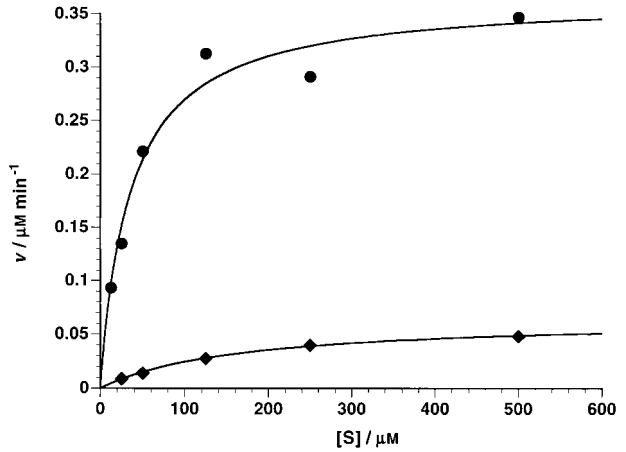

Figure 5. Michaelis–Menten plot (●: for initial rate V_0; ◆: for steady-state rate V_f) for the hydrolysis of **6** catalyzed by H8-1-2D5 (2.8 μM). Assays were performed at 37 °C in 50 mM HEPES, 80 μM NaCl, pH 7.8.

observed with serine proteases such as chymotrypsin, which catalyze the hydrolysis of amides and esters through the formation of an acyl intermediate.[20] Extrapolation of the linear portion (steady-state V_f) to time 0 gave the active site concentration of 4 μM, which was in good agreement with the experimental concentration of the antibody combining site.

Chemical modification of H8-2-6F11 and H8-1-2D5 acted on distinctly different residues. The hydrolytic activity of H8-2-6F11 was unaffected by treatment with diethyl pyrocarbonate, but treatment with phenylglyoxal or tetranitromethane resulted in 96% or 98% loss of catalytic activity, respectively. Identical treatment of H8-2-6F11 in the presence of inhibitor **5a** resulted in only 15% loss of activity. When H8-2-6F11 was treated with glycine ethyl ester and EDC a 33% reduction in its activity was observed. These results suggest the presence of a tyrosine and an arginine residue in the active site of H8-2-6F11. The tyrosine may act as a nucleophile in the catalytic process by forming an acyl intermediate; this is consistent with the antibody's burst kinetics behavior. The participation of a tyrosine residue in the esterolytic process through nucleophilic catalysis has been reported previously.[7k,21]

Conclusion

It has been suggested elsewhere[9b] that immunization with a zwitterionic hapten might serve as an alternative to heterologous immunization. Herein we have successfully synthesized a stable, zwitterionic hapten (**4**), which has both positively and negatively charged functional groups. Immunization of mice with **4** resulted in the generation of catalytic antibody H8-1-2D5, which exhibited a rate acceleration ($k_{cat}/k_{un} = 1.3 \times 10^5$) that was of about the same order of magnitude as that obtained by heterologous immunization ($k_{cat}/k_{un} = 1.5 \times 10^5$) using two structurally related haptens, **1** and **2**. Although the structures of the substrates **3** and **6** differ, these results suggest that both heterologous and homologous immunization with a zwitterionic hapten yield catalytic antibodies with comparable rate acceleration and multiple turnovers in the case of ester hydrolysis. Both strategies appear equally applicable to chemical reactions that involve general acid and base catalysis. However, in case the synthesis of a zwitterionic hapten proves to be too challenging, a heterologous immunization strategy may be easier to implement.

Experimental Section

General methods (synthesis): All reactions were carried out in oven-dried glassware under an argon atmosphere. Column chromatography was performed using 230–400-mesh silica gel (Merck). ^{1}H NMR and ^{13}C NMR spectra were recorded at 300 and 75 MHz respectively on a Bruker XL-300 spectrometer. The spectra were reported as δ downfield from tetramethylsilane. Melting points were determined with a Yanagimoto melting point apparatus and were not corrected. Infrared spectra were recorded on a Shimadzu 8000 FT-IR spectrometer. Mass spectra were obtained on JEOL JMS-SX/SX 102A and JEOL JMS AX 505H mass spectrometers.

Compound 8: *p*-Nitrobenzaldehyde (21 g, 140 mmol) was added slowly to dichlorophenylphosphine (13.6 mL, 100 mmol) and benzylcarbamate (15.2 g, 100 mmol) in acetic acid (350 mL). The mixture was heated under reflux for 1 h and cooled. The precipitate was collected by filtration and washed with ethanol and diethyl ether to give the product as a white solid (34.7 g, 81%), which was not purified further. M.p. 253–255 °C (decomp); ^{1}H NMR (300 MHz, [D$_6$]DMSO): $\delta = 8.4$–8.3 (m, 1H; NHCbz), 8.17 (d, $J = 9$ Hz, 2H; 2arom. CH (*p*-NO$_2$Ph)), 7.8–7.1 (m, 12H; 2arom. CH (*p*-NO$_2$Ph), 10arom. CH (Ph)), 5.20 (dd, $J = 10$, 16 Hz, 1H; PCH), 4.88 (dd, $J = 13$, 21 Hz, 2H; CH$_2$Ph); IR (KBr): $\tilde{\nu} = 3324$, 1726, 1524, 1236, 964 cm^{-1}; elemental analysis calcd (%) for $C_{22}H_{19}N_2O_6P$ (412.1): C 59.16, H 4.49, N 6.57; found: C 58.88, H 4.39, N 6.43.

Compound 9: A solution of compound **8** (5.55 g, 13 mmol), EDC (7.5 g, 39 mmol) and 4-dimethylamino pyridine (DMAP, 80 mg, 0.65 mmol) in methanol (100 mL) and dimethyl sulfoxide (10 mL) was heated under reflux for 11 h and then concentrated. Hexane and water were added to the residue. The precipitate was collected by filtration and washed with hexane, water, and a small amount of diethyl ether to give the product as a white solid (5.15 g, 90%). M.p. 227–230 °C; ^{1}H NMR (300 MHz, CDCl$_3$, TMS): $\delta = 8.05$ (d, $J = 9$ Hz, 2H; 2arom. CH (*p*-NO$_2$Ph)), 7.7–7.3 (m, 12H; 2arom. CH (*p*-NO$_2$Ph), 10arom. CH (Ph)), 6.10 (brs, 1H; NHCbz), 5.30 (dd, $J = 9$, 25 Hz, 1H; PCH), 5.07 (dd, $J = 12$, 18 Hz, 2H; CH$_2$Ph), 3.73 (d, $J = 11$ Hz, 3H; POCH$_3$); IR (KBr): $\tilde{\nu} = 3216$, 1724, 1520, 1348, 1250, 1214 cm^{-1}; elemental analysis calcd (%) for $C_{22}H_{21}N_2O_6P$ (426.1): C 60.00, H 4.81, N 6.36; found: C 60.16, H 4.96, N 6.29.

Compound 10: Sodium borohydride (10.0 g, 260 mmol) was added to a cooled (ice bath) suspension of **9** (13.2 g, 22 mmol), nickel chloride hexahydrate (11.4 g, 46 mmol) in methanol (150 mL), and chloroform (500 mL), over a period of 45 min. Stirring was continued overnight at room temperature. The mixture was concentrated, and the black precipitate was dissolved in HCl (10%). The acidic solution was basified by the

0947-6539/01/0717-3752 $ 17.50+.50/0 *Chem. Eur. J.* **2001**, *7*, No. 17

addition of conc. ammonium hydroxide and extracted with chloroform. The organic layer was dried over $MgSO_4$ and concentrated. The residue was purified by flash column chromatography, eluting with dichloromethane/ethyl acetate (1:3 v/v with 0–2% of ethanol) to give the product as a slightly yellow solid (3.05 g, 34%). M.p. 226–228 °C; ^{1}H NMR (300 MHz, $CDCl_3$, TMS): $\delta = 7.7-7.3$ (m, 10H; 10arom. C*H* (Ph)), 6.97 (dd, $J = 2$, 8 Hz, 2H; 2arom. C*H* (*p*-NH_2Ph)), 6.51 (d, $J = 8$ Hz, 2H; 2arom. C*H* (*p*-NH_2Ph)), 5.80 (br, 1H; N*H*Cbz), 5.2–4.9 (m, 3H; PC*H*, CH_2Ph), 3.70 (d, $J = 11$ Hz, 3H; POCH_3); IR (KBr) : $\tilde{\nu} = 3216$, 1702, 1630, 1522, 1284, 1256, 1222 cm^{-1}; elemental analysis calcd (%) for $C_{22}H_{23}N_2O_4P_2$ (410.4): C 64.38, H 5.65, N 6.83; found: C 64.50, H 5.70, N, 7.00; HRMS (FAB$^+$): calcd for $C_{22}H_{24}N_2O_4P_2$ $[M+H]^+$ 411.1474; found: 411.1479.

Compound 11: A solution of **10** (530 mg, 1.3 mmol), EDC (748 mg, 3.9 mmol), and 3,3′-dithiodipropionic acid (135 mg, 0.65 mmol) in chloroform (50 mL) was stirred at RT for 17 h. The mixture was washed with water, dried over $MgSO_4$ and concentrated. The residue was purified by flash column chromatography, eluting with dichloromethane/ethyl acetate (1:3 v/v with 0–2% of methanol) to give the product as a white solid (210 mg, 33%). ^{1}H NMR (300 MHz, $CDCl_3$, TMS): $\delta = 8.25$ (br s, 2H; PhN*H*CO), 7.7–7.1 (m, 28H; 28 arom. C*H*), 5.4–5.2 (m, 2H; PC*H*), 5.05 (AB q, $J_{AB} = 13$ Hz, $\Delta\tilde{\nu}_{AB} = 41$ Hz, 4H; CH_2Ph), 3.58 (d, $J = 11$ Hz, 6H; POCH_3), 3.14 (t, $J = 7$ Hz, 4H; CH_2S), 2.79 (t, $J = 7$ Hz, 4H; COCH_2); elemental analysis calcd (%) for $C_{50}H_{52}N_4O_{10}P_2S_2$ (995.0): C 60.35, H 5.25, N 5.63; found: C 60.00, H 5.25, N 5.33; HRMS (FAB$^+$): calcd for $C_{50}H_{53}N_4O_{10}P_2S_2$ $[M+H]^+$ 999.2678; found: 999.2687.

Hapten 4: Trimethylsilyl iodide (0.39 mL, 2.8 mmol) was added to a suspension of **11** (137 mg, 0.138 mmol) and 2-methyl-2-butene (0.88 mL, 8.3 mmol) in acetonitrile (15 mL). The mixture was stirred for 24 h and concentrated. The residue was washed with dichloromethane and dissolved in methanol. Dichloromethane and hexane were added to this solution to precipitate crude **12** as a yellow solid (88 mg, 91%). A mixture of **12** (88 mg, 0.126 mmol), dithioerythritol (58 mg, 0.378 mmol), and triethylamine (24 μL) in methanol (6 mL) was stirred at RT for 30 min and concentrated. The residue was dissolved in a small amount of methanol. Dichloromethane and hexane were added to the solution to precipitate the product as a colorless solid (86 mg, 98%). ^{1}H NMR (300 MHz, CD_3OD): $\delta = 7.6-7.1$ (m, 9H; 9 arom. C*H*), 4.23 (d, $J = 12$ Hz, 1H; PC*H*), 2.79 (t, $J = 6$ Hz, 2H; CH_2S), 2.66 (t, $J = 6$ Hz, 2H; COCH_2); ^{13}C NMR (75 MHz, CD_3OD): $\delta = 172.21$ (NH*C*O), 139.8 (arom. *C* (CHC_6H_4NH)), 135.56 (d, $J = 133.5$ Hz; arom. *C* (Ph)), 133.7 (d, $J = 9.3$ Hz; arom. *C* (Ph)), 132.3 (arom. *C* (CHC_6H_4NH)), 130.6 (arom. *C* (CHC_6H_4NH)), 129.8 (d, $J = 4.1$ Hz; arom. *C* (Ph)), 128.92 (d, $J = 12.4$ Hz; arom. *C* (Ph)), 120.7 (arom. *C* (CHC_6H_4NH)), 57.7 (d, $J = 91.0$ Hz; P*C*H), 41.8 (CH_2SH), 20.8 (NHCH_2); elemental analysis calcd (%) for $C_{16}H_{19}N_2O_3PS$ (350.4): C 54.85, H 5.47, N 8.00; found: C 54.65, H 5.40, N 7.95; HRMS (FAB$^+$): calcd for $C_{16}H_{20}N_2O_3P$ $[M+H]^+$ 351.0932; found: 351.0915.

Compound 13: A suspension of **8** (15.1 g, 35 mmol) in ethanol (250 mL) was warmed to 50 °C. Palladium/carbon (10%; 30 mg) and hydrazine hydrate (10 mL) were added successively. The mixture was heated under reflux for 4 h, and the precipitate was collected by filtration, washed with hexane and a small amount of ethanol, and dried to give a slightly gray solid (11.3 g, 82%). This compound was not purified further as it is insoluble in almost all organic solvents. M.p. 284–285 °C; ^{1}H NMR (300 MHz, NaOD/D_2O): $\delta = 7.5-6.8$ (m, 12H; 12 arom. C*H*), 6.58 (d, $J = 7$ Hz, 2H; 2 arom. C*H* (*p*-NH_2Ph), 4.6–4.9 (m, 3H; PC*H*, CH_2Ph); IR (KBr): $\tilde{\nu} = 3244$, 2596, 1724, 1544, 1516, 1244, 1036, 1022 cm^{-1}; elemental analysis calcd (%) for $C_{21}H_{21}N_2O_4P$ (396.4): C 63.63, H 5.34, N 7.07; found: C 63.93, H 5.37, N 7.27.

Compound 15: A suspension of **13** (11.3 g, 28.5mmol), glutaric anhydride (20 g, 170 mmol), and DMAP (180 mg, 1.4 mmol) in pyridine (200 mL) was heated under reflux for 2 h, filtered, and concentrated. When the residue was acidified with HCl (1M), the product was precipitated. The precipitate was washed with water and dried to give crude **14** as a white solid (12.7 g, 87%).

A suspension of crude **14** (255 mg, 0.5 mmol) and EDC (290 mg, 1.5 mmol) in a mixture of dichloromethane (2.5 mL) and methanol (2.5 mL) was heated under reflux for 7 h and then concentrated. The residue was dissolved in dichloromethane, washed with brine, and dried over $MgSO_4$. The organic layer was concentrated and purified by flash column chromatography, eluting with ethyl acetate/dichloromethane (25–50% ethyl acetate) to give **15** as a white solid (139 mg, 52%). M.p. 158–163 °C; ^{1}H NMR (300 MHz, $CDCl_3$, TMS): $\delta = 7.9-7.1$ (m, 14H; 14 arom. CH), 6.05 (br s, 1H; N*H*CO), 5.4–4.8 (m, 3H; PC*H*, CH_2Ph), 3.60 (d, $J = 11$ Hz, 3H; POCH_3), 2.45 (t, $J = 7$ Hz, 2H; COCH_2), 2.42 (t, $J = 7$ Hz, 2H; COCH_2), 2.05 (quint., $J = 7$ Hz, 2H; $CH_2CH_2CH_2$); IR (KBr): $\tilde{\nu} = 1732$, 1670, 1606, 1538, 1214, 1026 cm^{-1}; elemental analysis calcd (%) for $C_{28}H_{31}N_2O_7P$ (382.1): C 62.45, H 5.85, N 5.20; found: C 62.43, H 5.85, N 5.08.

Compound 14: A solution of **15** (270 mg, 0.5 mmol) and lithium hydroxide monohydrate (84 mg, 2.0 mmol) in a mixture of water (4 mL) and THF (15 mL) was stirred at RT for 19 h. The mixture was concentrated and acidified with HCl (1M) to pH 1. The precipitate was collected by filtration and washed with a small amount of water, diethyl ether, and dichloromethane to give the product as a white solid (252 mg, 99%), which was not purified further. M.p. 168–175 °C (decomp.); ^{1}H NMR (300 MHz, CD_3OD): $\delta = 7.8-7.2$ (m, 14H; 14 arom. CH), 5.2–4.9 (m, 3H; PC*H*, CH_2Ph overlapping with solvent's peak), 2.41 (t, $J = 7$ Hz, 2H; COCH_2), 2.38 (t, $J = 7$ Hz, 2H; COCH_2), 1.96 (t, $J = 7$ Hz, 2H; $CH_2CH_2CH_2$); IR (KBr): $\tilde{\nu} = 1714$, 1604, 1530, 1244 cm^{-1}; elemental analysis calcd (%) for $C_{26}H_{27}N_2O_7P$ (510.48): C 61.17, H 5.33, N 5.49; found: 60.87, H 5.23, N 5.40; HRMS (FAB$^+$): calcd for $C_{26}H_{28}N_2O_7P$ $[M+H]^+$ 511.1634; found: 511.1650.

Inhibitor 5: A suspension of **14** (122 mg, 0.24 mmol) and palladium/carbon (10%; 15 mg) in methanol (20 mL) was stirred at RT under a hydrogen atmosphere for 9 h. The suspension was filtered and the precipitate was washed with hot water. The filtrate was concentrated to give the product as a white solid (98 mg, 97%). M.p. 235–240 °C (decomp.); ^{1}H NMR (300 MHz, D_2O): $\delta = 7.4-7.1$ (m, 7H; 7arom. C*H*), 8.51 (d, $J = 8$ Hz, 2H; 2arom. C*H*), 4.32 (d, $J = 12$ Hz, 1H; PC*H*), 2.23 (t, $J = 7$ Hz, 2H; COCH_2), 2.08 (t, $J = 7$ Hz, 2H; COCH_2), 1.72 (quint., $J = 7$ Hz, 2H; $CH_2CH_2CH_2$); IR (KBr): $\tilde{\nu} = 3416$, 1668, 1604, 1544, 1440, 1202, 1132 cm^{-1}; elemental analysis calcd (%) for $C_{18}H_{21}N_2O_5P$ (376.3): C 57.45, H 5.62, N 7.44; found: C 57.07, H 5.42, N 7.24; HRMS (FAB$^+$): calcd for $C_{18}H_{20}N_2O_5P$ $[M+H]^+$ 375.1110; found: 375.1116.

Preparation of antigen: Hapten **4** (8 mg) was dissolved in a mixture of DMF (624 μL) and DMSO (156 μL), and the resulting solution was slowly added to a solution of maleimide–KLH or maleimide–BSA (approximately 10 mg each) in phosphate-buffered saline (PBS) (2.8 mL). This mixture was stirred gently for 8 h at RT. The hapten solution (KLH–**4** or BSA–**4**) was then dialyzed twice against PBS (1 L) at 4 °C. The concentrations of KLH–**4** and BSA–**4** were determined by Pierce BCA protein assay reagent to be 1.2 mg mL^{-1} and 1.5 mg mL^{-1}, respectively. The hapten/protein molecular ratio, estimated by measuring the absorbance at 250 nm (λ_{max} of hapten **4**), was 144:1 for KLH (assumed mol. wt. KLH = 10^6) and 37:1 for BSA. Conjugate KLH–**4** was used for immunization and conjugate BSA–**4** was used for ELISA experiments.

Antibody production and purification: Ten Balb/c mice each received an intraperitoneal injection of KLH–**4** conjugate (100 μg) emulsified in RIBI adjuvant (MPL and TDM emulsion, RIBI Immunology Research) on days 1 and 14 (boost no. 1). On day 24, serum was taken from the animals, and the titer was determined by ELISA. On day 35, the mouse with the highest titer received a second intravenous boost (boost no. 2) with 50 μg per mouse of hapten **4** dissolved in PBS (100 μL, without adjuvant).

Three days after boost no. 2, the spleen was taken from the mouse and the spleen cells were fused with 5×10^7 P3X63-Ag8.653 myeloma cells by a Shimadzu Somatic Hybridizer SSH-10 with an FTC-34D3 electrode (electrode distance 4.0 mm; frequency 1 MHz; primary AC voltage 80 V; initial time 10 s; pulse width 40 μs; pulse height (DC voltage) 920 V; electric field strength 2.30 kV cm^{-1}; secondary AC voltage 80 V; pulse repeat interval 1.0 s; number of pulses 1; pulse height (VDC) change +0 V; final time 10 s; AC voltage decrease rate 0%; adhesion intensifier off). Hybridoma cells were plated into six 96-well plates; each well contained 100 μL of HAT-RPMI 1640 with 20% fetal bovine serum and 5% Briclone (RioResearch, Ireland). After two weeks, the plates were analyzed by ELISA to detect antibody binding to BSA–**4** conjugate. All positive colonies were subcloned twice according to the standard protocols. All the cell lines which retained binding after subcloning were injected individually into pristane-primed Balb/c mice to generate ascites. The harvested ascites fluids were treated with a saturated ammonium sulfate (AS) solution to give a final concentration of 50% AS. The precipitated antibodies were dissolved in PBS and purified over a NAP 10 column (Pharmacia) before chromatographic purification. Protein G affinity chromatography (loaded onto the column in 20 mM phosphate buffer, pH 7.0, and eluted with 100 mM

glycine/HCl, pH 2.7) was performed and the fractions containing antibody were then subjected to mono Q chromatography (Pharmacia, linear salt gradient from 0 to 1M NaCl in 20mM Tris/HCl, pH 7.5) to yield purified antibody. The subclass of each antibody was determined with a monoclonal antibody isotyping kit (Amersham RPN 29).

Kinetic measurements: Purified monoclonal antibodies were dialyzed against assay buffer (50mM Mes, 80μM NaCl, pH 6.2; 50mM HEPES, 80μM NaCl, pH 7.8; 50mM CHES, 80μM NaCl, pH 9.0) and the concentration was determined by measuring the absorbance at 280nm. Assays were performed by HPLC (reversed-phase column, Waters μBondapak™ C18) with acetonitrile/H_2O (containing 0.1% TFA) using a 12:88 isocractic program. *o*-Acetamidophenol was used as an internal standard to calculate the amount of 5-[(4-hydroxyphenyl)amino]-5-oxopentanoic acid (**16**). All assays were performed at least in duplicate.

The catalytic antibodies were screened initially at 37°C in buffered solution (50mM Mes, 80μM NaCl, pH 6.2; 50mM HEPES, 80μM NaCl, pH 7.8; 50mM CHES, 80μM NaCl, pH 9.0) containing 5% dioxane, ester **6** (500μM), and antibody (10μM). The rates were determined by measuring the initial formation of 5-[(4-hydroxyphenyl)amino]-5-oxopentanoic acid (**16**) by HPLC. Antibodies found capable of catalyzing the hydrolysis were studied further.

The antibody-catalyzed hydrolysis rates of **6** in the presence of antibody (0.5–10μM) were measured as a function of substrate concentration under conditions identical to the initial screening. The concentration of substrate was varied from 25μM to 3.0mM to obtain at least six data points, and the observed rates were corrected for the rate of uncatalyzed hydrolysis (in the absence of antibody). The corrected rates were analyzed by nonlinear least-squares fitting of the initial rate against substrate concentration to a hyperbolic curve described by the Michaelis–Menten equation [Eq. (4)], in which v is initial velocity, [Ab] and [S] are the antibody and substrate concentrations, and k_{cat} and K_m are the catalytic rate and Michaelis constants, respectively. For antibodies showing kinetic burst, the progressive curves were fitted to Equation (3) and initial rates (V_0) and steady-state rates (V_f) were determined. V_0 and V_f were analyzed by applying the Michaelis–Menten equation.

$$v = k_{cat}[Ab][S]/(K_m + [S]) \quad (4)$$

The K_i of inhibitor **5** was determined by quantitation of the effect of the concentration of **5** on the velocity of the antibody-catalyzed hydrolysis of **6**. Rates obtained at fixed antibody and substrate concentrations were fitted to Equations (1) and (2).

Chemical modification of catalytic antibodies: Hydrolytic activities of the modified antibodies were assayed by using a modified antibody (0.5μM for H8-1-2D5, or 2μM for H8-2-6F11) and substrate **6** (1mM for H8-1-2D5, or 0.5mM for H8-2-6F11).

Histidine: Diethyl pyrocarbonate (25mM) (10μL) in phosphate buffer (50mM, pH 7.0) was added to an aqueous solution of the antibody (10μM) in phosphate buffer (50mM, pH 7.0) (500μL), and the mixture was stirred at RT for 1 h. The solution was dialyzed against 50mM HEPES, 80μM NaCl, pH 7.8, and the concentration was determined by Pierce BCA protein assay reagent.

Arginine: A mixture of phenylglyoxal (6mM; 10μL) in $NaHCO_3$ (125mM, pH 8.3) and antibody (10μM, 390μL) in the same buffer was stirred at RT overnight. The solution was dialyzed against 50mM HEPES, 80μM NaCl, pH 7.8, and the concentration was determined by Pierce BCA protein assay reagent.

Tyrosine: Tetranitromethane (200mM) dissolved in dioxane (5μL) was added to a solution of antibody (10μM) in HEPES (50mM, pH 7.8), and the mixture was stirred at RT for 1 h. The low molecular weight materials were removed by Micropure 3 (Amicon) column, the solution was dialyzed against 50mM HEPES, 80μM NaCl, pH 7.8, and the concentration was determined by Pierce BCA protein assay reagent.

Aspartate and glutamate: Glycine ethyl ester (2mM) and EDC (2mM) at 4°C to a solution of antibody (10μM) in phospate butter (50mM, pH 5.6), and the mixture was stirred at 4°C overnight. The low molecular weight materials were removed by Micropure 3 (Amicon) column, the eluent was dialyzed against 50mM HEPES, 80μM NaCl, pH 7.8, and the concentration was determined by Pierce BCA protein assay reagent.

[1] a) A. Tramontano, K. D. Janda, R. A. Lerner, *Science* **1986**, *234*, 1566; b) S. J. Pollack, J. W. Jacobs, P. G. Schultz, *Science* **1986**, *234*, 1570.

[2] a) R. A. Lerner, S. J. Benkovic, P. G. Schultz, *Science* **1991**, *252*, 659; b) P. G. Schultz, R. A. Lerner, *Science* **1995**, *269*, 1835; c) M. Blackburn, A. Datta, H. Denham, P. Wentworth, Jr., *Adv. Phys. Org. Chem.* **1998**, *31*, 250; d) A. J. Kirby, *Acta Chem. Scand.* **1996**, *50*, 203; e) P. Wentworth, K. D. Janda, *Curr. Opin. Chem. Biol.* **1998**, *2*, 138; f) D. Hilvert, *Annu. Rev. Biochem.* **2000**, *69*, 751.

[3] a) A. Tramontano, A. A. Amman, R. A. Lerner, *J. Am. Chem. Soc.* **1988**, *110*, 2282; b) J. W. Jacobs, P. G. Schultz, R. Sugasawara, M. Powell, *J. Am. Chem. Soc.* **1987**, *109*, 2174; c) S. J. Pollack, P. Hsiun, P. G. Schultz, *J. Am. Chem. Soc.* **1989**, *111*, 5961.

[4] a) K. D. Janda, D. Schloeder, S. J. Benkovic, R. A. Lerner, *Science* **1988**, *241*, 1188; b) S. J. Benkovic, J. A. Adams, C. L. Borderws, Jr., K. D. Janda, R. A. Lerner, *Science* **1990**, *250*, 1135; c) R. A. Gibbs, P. A. Benkovic, K. D. Janda, R. A. Lerner, S. J. Benkovic, *J. Am. Chem. Soc.* **1992**, *114*, 3528; d) Y.-C. J. Chen, T. Dannon, L. Sastry, M. Mubaraki, M. T. Martin, T. S. Angeles, R. Sugasawara, N. I. Aman, A. D. Napper, M. J. Darsley, R. I. Sanchez, P. Booth, R. C. Titmas, *J. Am. Chem. Soc.* **1994**, *116*, 6508; e) C. Gao, B. J. Lavey, C.-H. L. Lo, A. Datt, P. Wentworth, Jr., K. D. Janda, *J. Am. Chem. Soc.* **1998**, *120*, 2211; f) O. Ersoy, R. Fleck, A. Sinskey, S. Masamune, *J. Am. Chem. Soc.* **1998**, *120*, 817.

[5] a) K. D. Janda, M. I. Weinhouse, D. M. Schloeder, R. A. Lerner, S. J. Benkovic, *J. Am. Chem. Soc.* **1990**, *112*, 1274; b) K. D. Janda, M. I. Weinhouse, T. Dannon, K. A. Pacelli, D. M. Schloeder, *J. Am. Chem. Soc.* **1991**, *113*, 5427; c) M. T. Martin, A. D. Napper, P. G. Schultz, A. R. Ress, *Biochemistry* **1991**, *30*, 9757; d) D. W. Landry, K. Zhao, G. X.-Q. Yang, J. A. Ashley, T. M. Jones, D. A. Mcleod, D. M. Schloeder, M. I. Weinhouse, R. A. Lerner, R. A. Gibbs, P. A. Benkovic, R. Hilhorst, S. J. Benkovic, *J. Am. Chem. Soc.* **1991**, *113*, 291; e) K. D. Janda, S. J. Benkovic, R. A. Lerner, *Science* **1989**, *244*, 437; f) D. S. Tawfik, R. R. Zemel, R. Arad-Yellin, B. S. Green, R. Chap, M. Sela, Z. Eshhar, *Proc. Natl. Acad. Sci. USA* **1993**, *90*, 373; g) H. Miyashita, Y. Karaki, M. Kikuchi, I. Fujii, *Proc. Natl. Acad. Sci. USA* **1993**, *90*, 5337; h) Y. Iwabuchi, H. Miyashita, R. Tanimura, K. Kinoshita, M. Kikuchi, I. Fujii, *J. Am. Chem. Soc.* **1994**, *116*, 771; i) H. Miyashita, T. Hara; R. Tanimura, F. Tanaka, M. Kikuchi, I. Fujii, *Proc. Natl. Acad. Sci. USA* **1994**, *91*, 6045; j) I. Fujii, F. Tanaka, H. Miyashita, R. Tanimura, K. Kinoshita, *J. Am. Chem. Soc.* **1995**, *117*, 6199; k) G. W. Zhou, J. Guo, W. Huang, R. J. Fletterick, T. S. Scanlan, *Science* **1994**, *265*, 1059.

[6] a) P. Wirsching, J. A. Ashley, C.-H. L. Lo, K. D. Janda, R. A. Lerner, *Science* **1995**, *270*, 1775; b) J. Wagner, R. A. Lerner, C. F. Barbas III, *Science* **1995**, *270*, 1797; c) C. F. Barbas III, C. Rader, D. J. Segal, B. List, J. M. Turner, *Adv. Protein Chem.* **2001**, *55*, 317.

[7] a) G. M. BacBeath, D. Hilvert, *Chem. Biol.* **1996**, *3*, 433; b) H. Wade, T. S. Scanlan, *Annu. Rev. Biophys. Biomol. Struct.* **1997**, *26*, 461; c) G. W. Zhou, J. Guo, W. Huang, R. J. Fletterick, T. S. Scanlan, *Science* **1994**, *265*, 1059; d) B. Golinelli-Pimpaneau, B. Gigant, T. Bizebard, J. Navaza, P. Saludjian, R. Zemel, D. S. Tawfik, Z. Eshhar, B. S. Green, M. Knossow, *Structure* **1994**, *2*, 175; e) J. B. Charbonnier, E. Carpenter, B. Gigant, B. Golinelli-Pimpaneau, Z. Eshhar, B. S. Green, M. Knossow, *Proc. Natl. Acad. Sci. USA* **1995**, *92*, 11721; f) J.-B. Charbonnier, B. Golinelli-Pimpaneau, B. Gigant, D. S. Tawfik, R. Chap, D. G. Schindler, S. H. Kim, B. S. Gree, Z. Eshhar, M. Knossow, *Science* **1997**, *275*, 1140; g) B. Gigant, J. B. Charbonnier, Z. Eshhar, B. S. Green, M. Knossow, *Proc. Acad. Natl. Sci. USA* **1997**, *94*, 7857; h) J. B. Charbonnier, B. Gigant, B. Golinelli-Pimpaneau, M. Knossow, *Biochimie* **1997**, *79*, 653; i) O. Kristensen, D. G. Vasslyev, F. Tanaka, K. Morikawa, I. Fujii, *J. Mol. Biol.* **1998**, *281*, 501; j) G. J. Wedemayer, P. A. Patten, L. H. Wang, P. G. Schultz, R. C. Stevens, *Science* **1997**, *276*, 1665; k) B. Gigant, T. Tsumuraya, I. Fujii, M. Knossow, *Structure* **1999**, *7*, 1385.

[8] G. Fischer, in *Enzyme Mechanisms* (Eds.: M. I. Page, A. Williams), The Royal Society of Chemistry, London, **1987**, pp. 229–239.

[9] a) H. Suga, O. Ersoy, T. Tsumuraya, J. Lee, A. J. Sinskey, S. Masamune, *J. Am. Chem. Soc.* **1994**, *116*, 487; b) H. Suga, O. Ersoy, S. F. Williams, T. Tsumuraya, M. N. Margolies, A. J. Sinskey, S. Masamune, *J. Am. Chem. Soc.* **1994**, *116*, 6025; c) H. Suga, O. Ersoy, S. F. Williams, T. Tsumuraya, M. N. Margolies, A. J. Sinskey, S. Masamune, *J. Am. Chem. Soc.* **1994**, *116*, 8432; d) T. Tsumuraya, H.

  0947-6539/01/0717-3754 $ 17.50+.50/0

Suga, S. Meguro, A. Tsunakawa, S. Masamune, *J. Am. Chem. Soc.* **1995**, *117*, 11390.
[10] a) G. H. Biram, *J. Org. Chem.* **1974**, *39*, 209; b) J. W. Huber, M. Middlebrooks, *Synthesis* **1977**, 883; c) J. Oleksyszyn, R. Tyka, P. Mastalerz, *Synthesis* **1978**, 479; c) J. Oleksyszyn, E. Gruszecka, P. Kafarski, P. Mastalerz, *Monatsh. Chem.* **1982**, *113*, 59.
[11] G. Köhler, C. Milstein, *Nature* **1975**, *256*, 495.
[12] M. M. S. Lo, T. Y. Tsong, M. K. Conrad, S. M. Strittmatter, L. D. Hester, S. H. Snyder, *Nature* **1984**, *310*, 792.
[13] In a competitive ELISA experiment the observed K_d values do not necessarily reflect the absolute K_d of an antibody because of the avidity effect of divalent antibody molecules. Nevertheless, these values should be useful for comparison.
[14] B. Friguet, A. F. Chaffotte, C. Djavadi-Ohaniance, M. E. Goldberg, *Imumunol. Methods* **1985**, *77*, 305.
[15] J. W. Williams, J. F. Morrison, *Methods Enzymol.* **1979**, *63*, 437.
[16] K. Takahashi, *J. Biol. Chem.* **1968**, *243*, 6171.
[17] E. W, Miles, *Methods Enzymol.* **1977**, *47*, 431.
[18] P. Cuatrecasas, S. Fuchs, C. G. Anfinsen, *J. Biol. Chem.* **1968**, *243*, 4787.
[19] If a tyrosine were involved in the catalytic process, an almost complete loss of activity should have been observed (as in H8-2-6F11). This partial loss of activity, however, may stem from a conformational change in the protein induced by modified amino acid residues distant from the active site.
[20] B. S. Hartley, B. A. Kilby, *Biochem. J.* **1954**, *56*, 288.
[21] a) T. S. Angeles, R. G. Smith, M. J. Darsley, R. Sugasawara, R. I. Sanchez, J. Kenten, P. G. Schultz, M. T. Martin, *Biochemistry* **1993**, *32*, 12128; b) M. T. Martin, *Drug Discovery Today* **1996**, *1*, 239.

Received: November 13, 2000
Revised: April 30, 2001 [F2865]

  0947-6539/01/0717-3755 $ 17.50+.50/0